

UDK 553.689:622.785

Electrical Characterization and Impedance Response of Lanthanum Doped Barium Titanate Ceramics

D.Mančić¹, V.Paunović¹, M.Vijatović², B.Stojanović², Lj.Živković^{1*)}

¹ Faculty of Electronic Engineering, University of Niš, A.Medvedeva 14, Niš, Serbia

² Institute for Multidisciplinary Research, University of Belgrade, Kneza Višeslava 1a, Belgrade, Serbia

Abstract:

The dielectric permittivity and dissipation factor of La-doped and undoped BaTiO₃ were investigated as a function of frequency and temperature. The impedance response was used to study the electrical properties of La-doped BaTiO₃ over the temperature range from room temperature (RT) to 350 °C. La-doped and undoped BaTiO₃, obtained by a modified Pechini method, were sintered in air at 1300 °C for 2 and 16 hours. The impedance spectra were analyzed in terms of equivalent circuits involving resistors, capacitors and constant phase elements (CPE). The most suitable electrical circuit for the interpretation of experimental results is found to be the equivalent circuit consisting of resistors and CPE elements which replace the capacitor elements. The contribution of grain boundary resistance to the total resistance of a system is remarkable at low temperature. Dielectric permittivity of doped BaTiO₃ was in the range of 8000 to 12000 at 1 kHz and the dissipation factor was less than 1%.

Keywords: La-doped BaTiO₃, Impedance spectroscopy, Equivalent circuit, Dielectric permittivity.

1. Introduction

Barium titanate based ceramics is one of the most investigated ferroelectric ceramics because of its numerous practical applications [1,2]. The electrical and dielectric properties of ceramics can be modified using various type of additive as well as processing procedures. Among the additive/dopants lanthanum (La) is the most efficient in raising the dielectric permittivity of modified BaTiO₃ ceramics. A small amount of La³⁺ ions, which exclusively replace Ba sites in the perovskite structure of BaTiO₃, leads to the formation of a n-type BaTiO₃ semiconductor, if the samples are heated in a reducing or argon atmosphere. However, samples sintered in air atmosphere are electrically insulating [3,4]. Taking into consideration the complex structure of polycrystalline ceramics which is composed of grains, grain boundaries, second phases, pores and electrode-ceramics surfaces, it is not possible to distinguish the resistivity or capacitive contributions of each of these elements to the overall resistivity or capacitance of ceramics by simple DC measurements. From this point of view the use of impedance spectroscopy (IS), for evaluating the contribution of a particular

*) Corresponding author: ljivkovic@elfak.ni.ac.yu

component and its effects on the overall electrical properties of ceramics, is of great importance [5-8]. In modified ceramics, high resistive grain boundaries are of great technological significance, since they represent the regions that are responsible for the PTC effect and the regions where segregation of the additive occurs.

In order to extract the resistance and capacitance values of bulk and grain boundary regions it is necessary to model the impedance data in terms of an equivalent electrical circuit that contains the bulk and grain boundary elements. There are numerous equivalent circuits [9-12], but almost all of them are based on the equivalent circuit that includes two parallel resistor-capacitor (RC) elements connected in series. To describe additional features, such as deviation from the ideal capacitor behaviour, constant phase elements (CPE) are also included. CPE elements are used to explain the phenomena occurring in the interface regions from one side, and the phenomena associated with the nonhomogeneity, diffusion processes or stresses on the other side [7,13]. The purpose of this work is to investigate the impedance response of La-doped BaTiO₃ using a) a basic electrical circuit with two (RC) elements and b) equivalent electrical circuits with CPE elements. The multidimensional Simplex identification algorithm [14] and in-house made software were used for fitting and simulation process of IS data. Good agreement between the experimental and simulated values was obtained with the equivalent circuit with two parallel sets of (RCPE) elements connected in series. The DC measurements of dielectric permittivity (ϵ_r) and dissipation factor ($\tan\delta$) of ceramics have also been done.

Experiments and methods

Lanthanum doped BaTiO₃ samples, with 0.3 mol% La and 0.01 mol% Mn (denoted as La-BT in the text) were prepared from an organometallic complex based on the modified Pechini procedure [15,16]. For comparison purposes samples free of La and Mn were prepared in the same manner. The modified Pechini process was carried out as a three stage process for the preparation of a polymeric precursor resin. The detailed procedure was reported earlier herein [16]. After calcination at 700°C and milling, the powder was pressed at 98 MPa and sintered in air at 1300°C for 2 and 16 hours. The microstructures of as sintered samples were observed by a scanning electron microscope JEOL, JSM-5300 equipped with an energy dispersive spectrometer (EDS system). Prior to electrical measurements, silver paste was applied on both flat surfaces of specimens. Capacitance, dissipation factor and impedance measurements were done using an Agilent 4284A precision LCR meter in the frequency range of 20 to 10⁶ Hz. Variation of the dielectric permittivity with temperature was measured in temperature interval from 20° to 180°C.

Impedance spectra were modeled using three different electrical circuits and identification of the associated parameters was performed by a multidimensional Simplex algorithm using in-house made software [17]. All measurements were executed in air at room temperature (RT), 200°, 330° and 350°C.

Results and discussion

Microstructure characteristics

The density of doped samples was over 95% of theoretical density (TD). La-doped BaTiO₃ ceramics sintered for 2 hours exhibited a fairly uniform microstructure with grain size ranging from 1-3 μm as shown in Fig.1a. The microstructure of specimens sintered for 16 hours showed quite significant grain growth with a varied grain size. Besides a small amount of grains of 1 μm , most of grains were approximately 3-5 μm in size (Fig.1b). The undoped

BaTiO₃, obtained by the same modified Pechini method, showed a non uniform grain size distribution from 0.5-15 μm, (Fig.1c.).

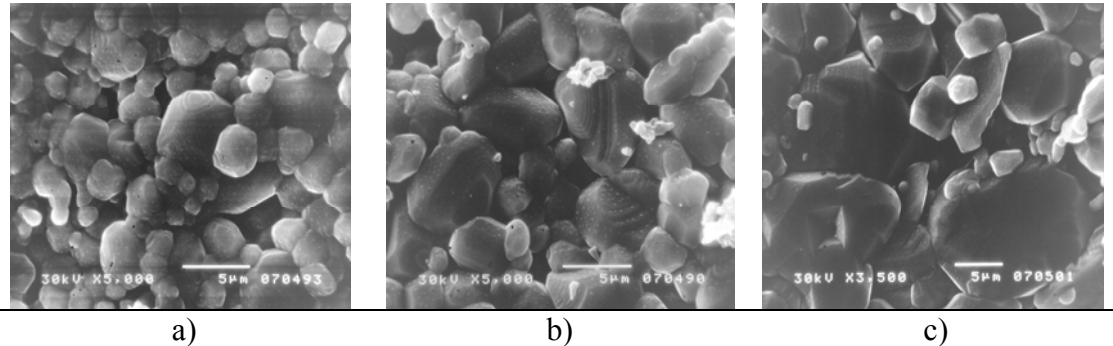


Fig. 1 SEM images of La-BT samples sintered at 1300°C for a) 2 hours, b) 16 hours and c) SEM images of undoped BaTiO₃ sample sintered for 16 hours.

In order to investigate the chemical homogeneity of doped samples, EDS analysis with a beam controller was done across the whole surface of specimens and except Ba- Lα and Ti-Kα peaks no other peaks were found (Fig.2).

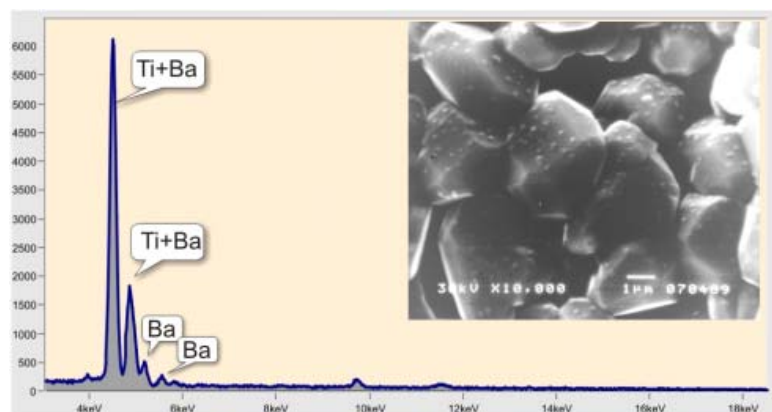


Fig.2. EDS spectrum of La-BT samples sintered at 1300°C for 2 hours.

Thus homogeneous incorporation and equal distribution of La and Mn throughout the doped specimens can be assumed.

Electrical characteristics

Regarding the electrical resistivity, all samples were electrically insulating with a resistivity of 10⁸ Ωcm at room temperature. Because of the high resistivity it is believed that the titanium vacancy compensation mechanism is exclusively involved during the incorporation of La into the BaTiO₃ matrix.

Since the key properties of ferroelectric ceramics are the dielectric permittivity and dissipation factor these values were measured as a function of frequency and temperature and the results are presented in Figs. 3-5.

As can be seen in Fig.3a La-BT, that was sintered for 2 hours, exhibits a high dielectric

permittivity, almost 12000 at room temperature and 1 kHz. The Pechini method of preparation has the advantage in raising the permittivity of modified barium titanate, compared with the samples obtained by conventional solid state sintering which showed a permittivity of 3000-4000 [18].

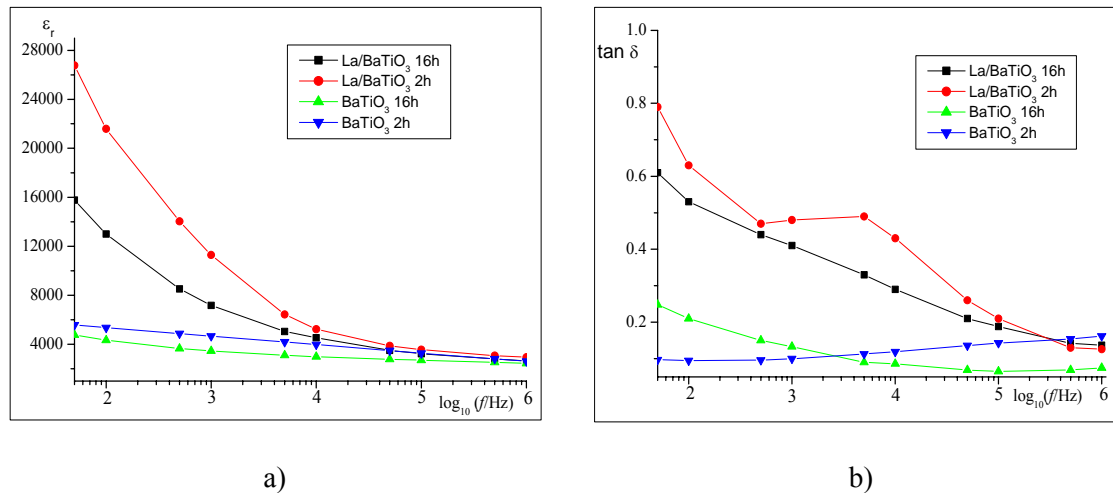


Fig. 3. Frequency dependence of a) dielectric permittivity (ϵ_r) and b) dissipation factor ($\tan \delta$) for undoped and La doped BaTiO_3 measured at 20°C .

A strong increase of the dissipation factor, in a low frequency region, was detected for doped BaTiO_3 contrary to undoped BaTiO_3 for which the dissipation factor is essentially independent of frequency (Fig.3b). Permittivity of La-BT sintered for 2 hours, measured at several temperatures, (Fig.4) indicates the high frequency plateau associated with the bulk response.

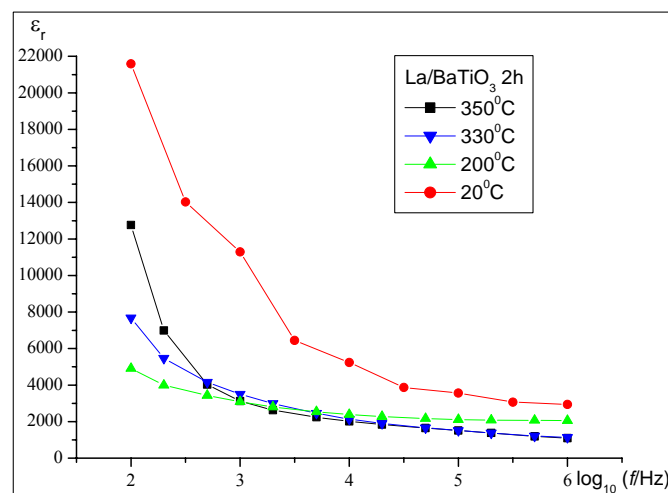


Fig. 4. Dielectric permittivity as a function of frequency for La-BT sintered for 2 hours measured at several temperatures.

All the investigated samples follow the Curie-Weiss behaviour as can be seen in Fig.5. The Curie temperature (T_C) for La-doped samples is shifted towards low temperatures, being around 105°C for the specimen sintered for 2 hours. Another interesting characteristic

of La-BT sintered for 2 hours is that the dielectric permittivity gradually increases with temperature and ϵ_{max} at T_C reaches 37000.

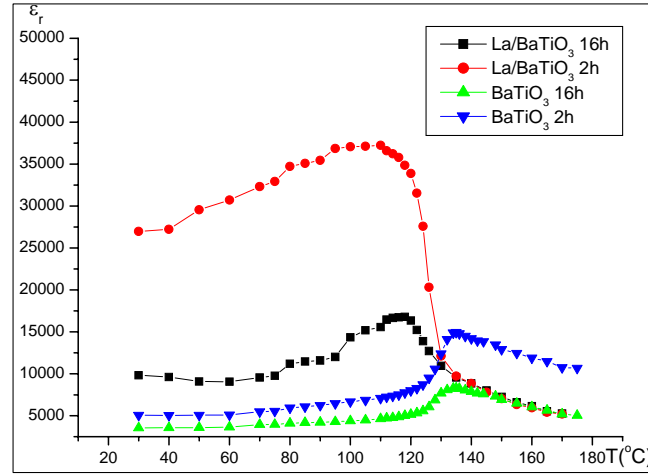


Fig. 5. Dielectric permittivity in function of temperature for undoped and La doped BaTiO₃ sintered for 2 and 16 hours

The occurrence of a broad permittivity maxima for doped samples pointed out the diffuse phase transformation. One of the possible explanations for a considerably high dielectric permittivity in specimens sintered for 2 hours is that the long term sintering of 16 hours, intensifies the diffusion of La into the BaTiO₃ core, thus leading to the decrease of ferroelectric regions and consequently to the decrease of dielectric permittivity. The impedance measurements are focused on the analysis of doped samples sintered for 2 hours.

Impedance characteristics

For modeling the impedance spectra it is necessary to use the equivalent circuit whose parameters represent the different parts in ceramics microstructure, primarily bulk and grain boundary regions. There are numerous equivalent circuits consisting of a set of resistors, capacitors and CPE elements [4,8]. The goal is to find the equivalent circuit, as simple as possible, which best fits the experimental results in the entire range of frequency. For the presentation of IS data, the complex impedance, Z'' vs. Z' plots are the most commonly used plots, although the other three complex formalisms, such as relative electric modulus M^* , admittance Y^* and relative permittivity ϵ^* may be used as well. The relationship between them is given as:

$$M^* = j\omega C_0 Z^* = j\omega C_0 (1/Y^*) = 1/\epsilon^* \quad (1)$$

where $\omega = 2\pi f$ is the angular frequency and f is the applied frequency in Hz, $C_0 = \epsilon_0 S/d$ is the vacuum capacitance of the empty cell between electrodes, $\epsilon_0 = 8.85 \times 10^{-12}$ F/m is the permittivity of vacuum, S and d are the cross-sectional area and thickness of the sample, respectively.

For the analysis of our experimental spectra, we started with several equivalent circuits. Some of these circuits were complex ones, such as an equivalent circuit with two parallel (RCCPE) elements but without a substantial improvement in the simulation of the obtained results. Thus, we selected two rather simple equivalent circuits, which in our opinion

gave a very good simulation of the obtained IS data, together with the basic (RC) circuit, just for comparison purposes. The equivalent circuits used in this examination are presented in Fig.6. In this analysis the contribution associated with the sample-electrode interface to the overall electrical response is neglected.

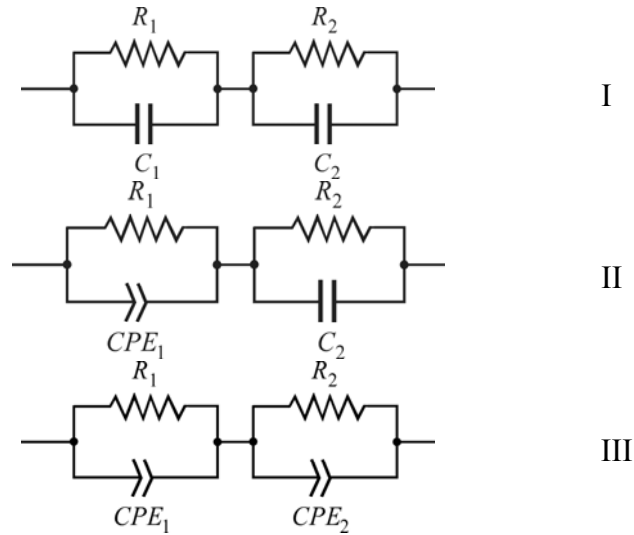


Fig.6. Equivalent electrical circuits used to model IS data from a La-BT ceramic.

The circuit (I) is the most representative model and the basic one. In this case two parallel RC elements connected in series represent ideal “Debye” like behavior and the complex impedance is given as follows:

$$Z^* = Z' - Z'' = \frac{1}{1/R_1 + j\omega C_1} + \frac{1}{1/R_2 + j\omega C_2} \quad (2)$$

R_1 and C_1 refer to the resistive and capacitive component of the bulk region and R_2 and C_2 to the resistive and capacitive component of the grain boundary.

For non ideal “Debye” like behavior, which is the most real case concerning ceramic materials, the arc in complex impedance Z'' vs. Z' plots is depressed with its centre below the real axis. Therefore a constant phase element (CPE) may be used to replace the capacitor, or as an addition to resistor and capacitor in the circuit. In some cases these deviations from ideal behaviour are often ignored. The impedance of a CPE element is given as:

$$Z_{\text{CPE}}^* = [A(j\omega)^n]^{-1} \quad (3)$$

where A is a constant that is independent of frequency and n is an exponential index which is a measure of arc-depression. For ideal “Debye” like behavior, the constant $n=1$ and CPE represents an ideal capacitor with a value $C=A$. The n value below unity indicates that a capacitor is frequency-dependent. For $n=0$, the CPE acts as a pure resistor with a value of $R=1/A$. The calculation of parameter n is described in detail in [13].

In circuit (II), CPE is used instead of the capacitive component (bulk region) C_1 , and the total impedance for this configuration is given as:

$$Z^* = Z' - Z'' = \frac{1}{1/R_1 + A_1(j\omega)^{n_1}} + \frac{1}{1/R_2 + j\omega C_2} \quad (4)$$

In circuit (III) two CPEs replace both capacitive components, C_1 corresponding to bulk and C_2 to the grain boundary region. The impedance, corresponding to this equivalent circuit, takes the form:

$$Z^* = Z' - Z'' = \frac{1}{1/R_1 + A_1(j\omega)^{n_1}} + \frac{1}{1/R_2 + A_2(j\omega)^{n_2}} \quad (5)$$

In the fitting procedure, it is necessary, firstly, to take the starting values R_1 and R_2 for each component in the circuit and afterwards to find the more appropriate values. For circuit (I), the R_1 value was estimated from the diameter of the arc in the Z^* plot and C_1 from the relationship $\omega_{max}RC=1$, where $\omega_{max}=2\pi f_{max}$ and f_{max} is the frequency at the top of the arc. In a similar way, R_2 and C_2 were estimated from the arcs in the M^* plot and from the impedance and modulus formalism combination as reported in [5]. The fitting software refined the values of R and C to obtain the best fit with the experimental results. The input values of A and n in circuits (II) and (III) were estimated by analyzing the measured data for Y' , as reported in [7].

The model's parameters such as R_1 , C_1 , n_1 and so on, were calculated using the Simplex method in which the function's calculation, without the calculation of derivatives, is only required. The Simplex method is time consuming, and not very efficient, regarding the number of functional calculations, however, in our case for the determination of optimal circuit's parameters (the equations with six unknown variables), the Simplex method proved to be more than effective. Using this method, realized with Matlab tools [17], the approximated values of required parameters were obtained by fitting the vector with the unknown parameters as variables: R_1 , C_1 and R_2 , C_2 in Eq. (2), R_1 , A_1 , n_1 and R_2 , C_2 in Eq. (4) and R_1 , A_1 , n_1 and R_2 , A_2 , n_2 in Eq. (5).

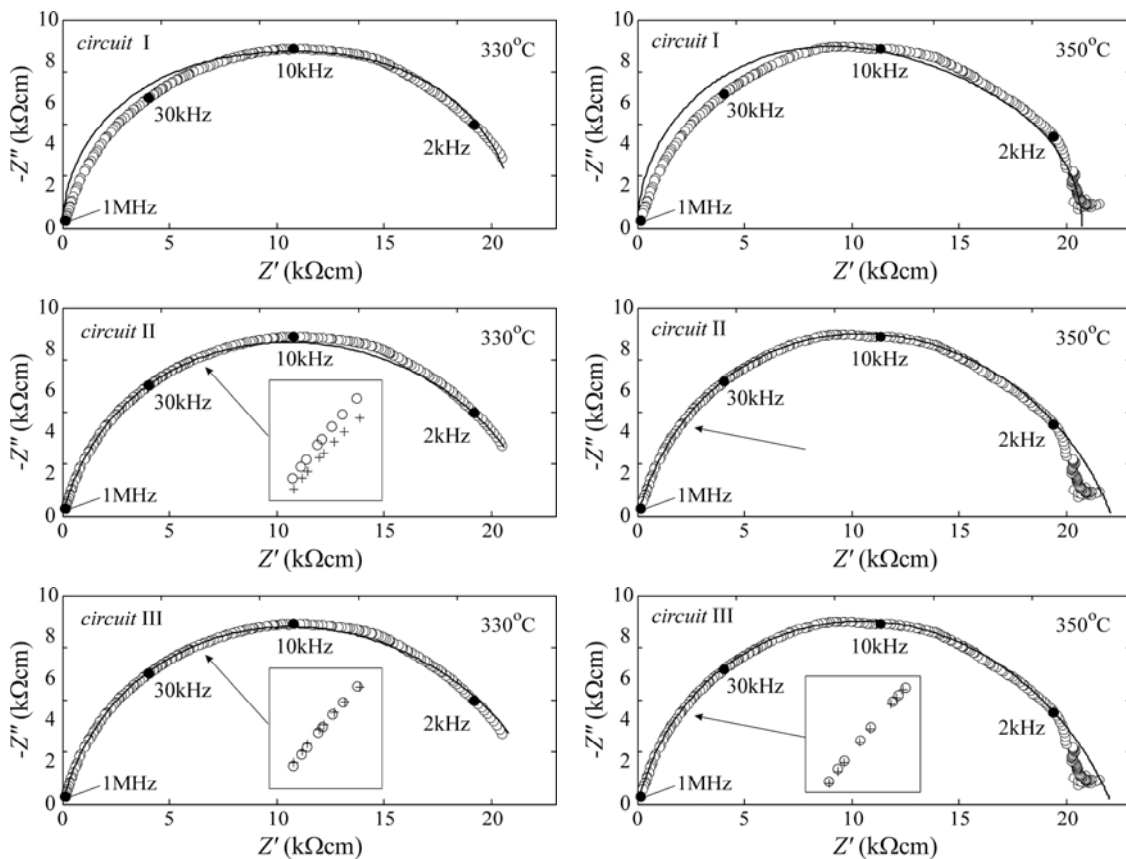


Fig.7. Measured (circles) and simulated (solid lines) *ac* complex-plane impedance plots for La-BT for equivalent circuits (I, II and III) at a) 330°C and b) 350°C. Selected frequencies are shown as filled circles.

All impedance measurements were done at temperatures far above the Curie

temperature. However, because of the limited frequency range of equipment, an incomplete arc appears at 200°C, whereas, the spectra obtained at higher temperatures showed satisfactory quality.

The two complex plane plots, Z'' vs. Z' , corresponding to the above models, for 330 and 350°C, are presented in Fig.7. Modeling was performed in the same way for all three equivalent circuits, i.e. using Eqs. (3), (4) and (5) and the values of the elements in the equivalent circuits were extracted from Z'' vs. Z' plots. Typical results from the fitting procedure using equivalent circuits are shown as solid lines.

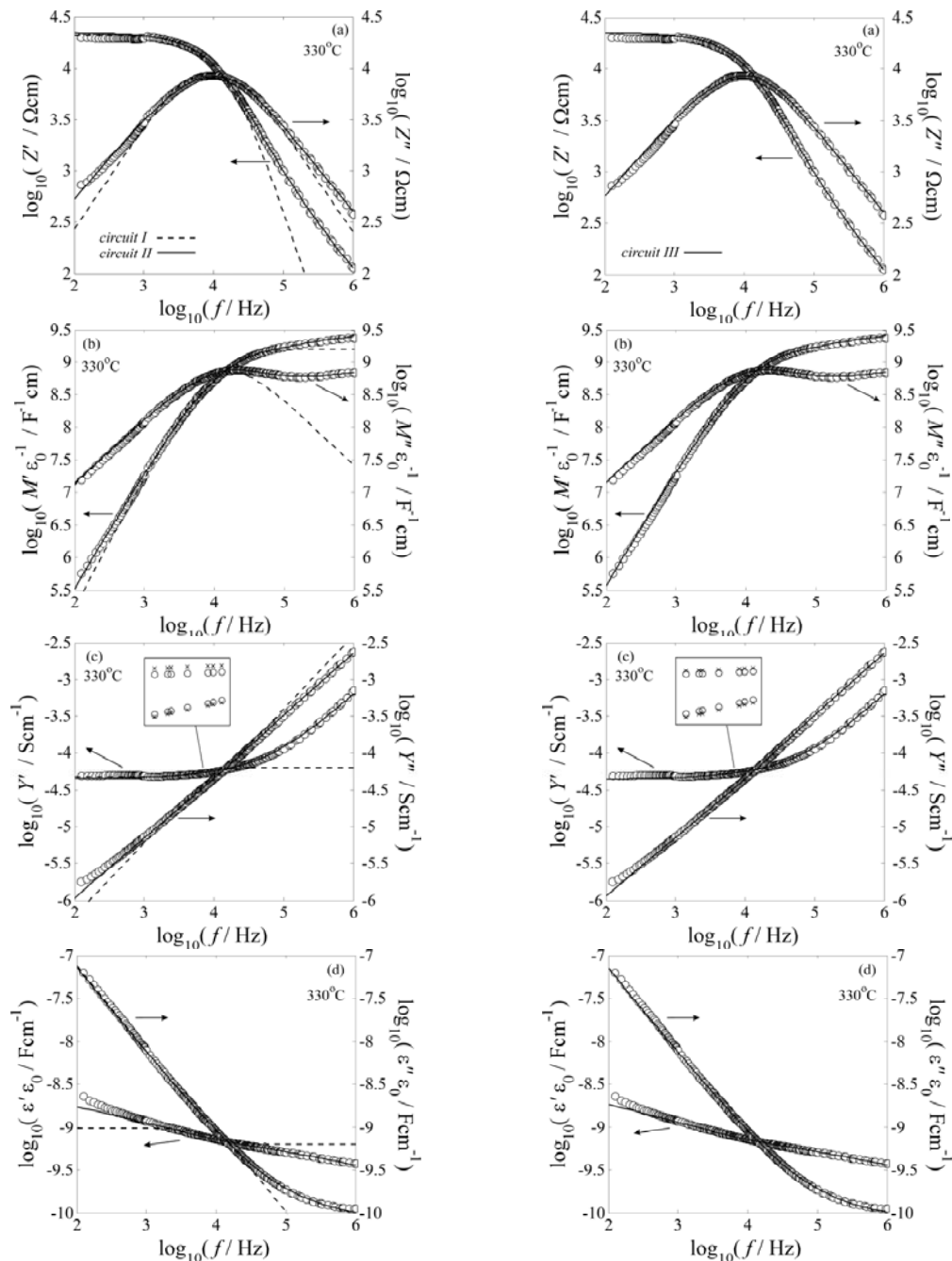


Fig. 8. Normalized log-log spectroscopic plots of the real and imaginary parts at 330°C of a) Z^* , b) M^* , c) Y^* and d) ε^* , measured (circles), and the best-fit simulated for equivalent circuits given in Fig.6 (solid and dashed lines).

A fairly good agreement has been achieved between experimental and simulated values using equivalent circuits (II) and (III), although, the best fitting has been obtained using circuit (III). To prove that the proposed equivalent circuits (II) and (III) are correct not only for Z^* plots but as well as for all four formalisms, the normalized log-log spectroscopic plots of the real and imaginary component for Z^* , M^* , Y^* and ε^* in function of frequency are modeled and presented in Figs. 8 and 9.

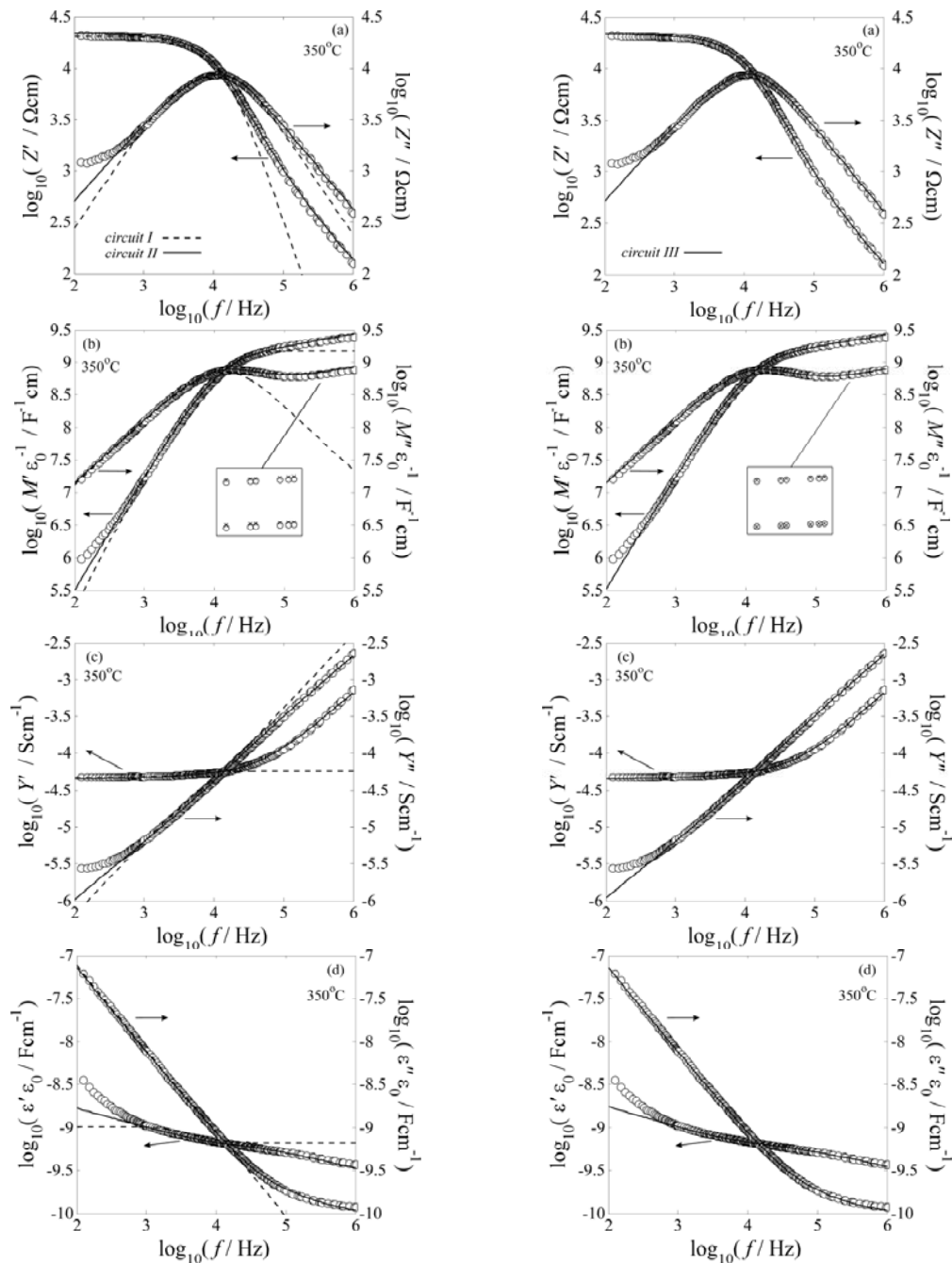


Fig.9. Normalized log-log spectroscopic plots of the real and imaginary parts for the data obtained at 350°C of a) Z^* , b) M^* , c) Y^* and d) ε^* , measured (circles) and the best-fit simulated for equivalent circuits given in Fig.6 (solid and dashed lines).

The greatest deviations at lower and higher frequencies, between experimental and simulated values, were observed for circuit (I), compared with the results obtained for other two circuits. The plots given in Figs. 8,9 pointed out that the model described with circuit (III) is best suited for all analyzed formalisms. Less fit simulation is observed only at a frequency below 200 Hz. The fitted values used for circuit (III) are presented in Tab. I.

Tab. I. Fitted values of resistance and CPE parameters for circuit III given in Fig. 6.

$T(^{\circ}\text{C})$	<i>Bulk region</i>			<i>Grain boundary</i>		
	$R_1(\Omega)$	CPE_1		$R_2(\Omega)$	CPE_2	
		$A_1(\text{nF})$	n_1		$A_2(\text{nF})$	n_2
200	1.51×10^4	4.60	0.95	2.20×10^6	4.90	0.85
330	1.59×10^3	4.33	0.95	2.0×10^4	2.90	0.89
350	1.57×10^3	63.16	0.76	1.88×10^4	2.70	0.95

Although the equivalent circuit (III) contains a large number of fitting parameters (six parameters), all of them are allowed to vary simultaneously using an in-house software based on the Simplex method. Instead of using a fixed value of n , obtained from the lowest temperature data, (which is common in some cases) we performed the calculation and refinement of n for each temperature. The satisfactory fitting of IS data, with different n values, indicates that the dependence capacitance on frequency is different in intensity for bulk and grain boundary regions. We believe that CPE_1 and CPE_2 elements with $n \geq 0.85$, obtained at 200° and 330°C, correspond mainly to capacitors, whereas CPE_1 with $n = 0.76$ at 350°C corresponds both to the resistive and capacitive behaviour of the bulk region. As can be seen from Tab. I, the n values are different at different temperatures. It is not necessary to say that n depends on temperature, it is rather that IS data, obtained at a higher temperature, highlights better the difference between grain and grain boundary behavior. According to the data given in Tab. I the contribution of grain boundary resistance to the total resistance of ceramics is dominant at low temperature and its effect is less pronounced at 330 and 350°C.

The results shown in Figs. 8 and 9 illustrate the validity of the proposed equivalent circuits as well as the successful application of the in-house software that enables assessment of the most plausible model. Although circuit (III) has a large number of fitting parameters, compared to the other two models, the use of this circuit gives the best fitting of the impedance response in almost the entire frequency range.

Conclusion

Dielectric permittivity of doped BaTiO₃, obtained by the modified Pechini method, was in the range of 8000 to 12000 at 1 kHz and dissipation factor was less than 1%. The impedance results were interpreted in terms of three different equivalent circuits involving capacitors, resistors and CPE elements. Good agreement between experimental and simulated results was obtained using an equivalent circuit with two parallel (RCPE) sets connected in series. The circuit parameter n , being ≥ 0.85 at 200° and 330°C, highlights the capacitive nature of bulk and grain boundary elements. The low value of n at 350°C pointed out the dual behavior of the grain's interior. The different values of n were associated with different frequency dependence of the capacitance of bulk and grain boundary regions. The participation of grain boundary resistance in the overall resistance of a system is dominant at 200°C and at higher temperatures is slightly higher than the resistance of the bulk region.

Acknowledgements

This research is part of the project "Investigation of the relation in triad: synthesis-structure-properties for functional materials" (No.142011G), project COST 539 and project "Synthesis, characterization and activity of organic and coordination composition and their application in (bio) nanotechnology" (No.142010). The authors gratefully acknowledge the financial support of the Serbian Ministry for Science for this work.

References

1. G.H.Haertling, J. Am. Ceram. Soc., 82 (1999) 797.
2. A.J.Moulson, J.M.Herbert, Electroceramics, Willey Press, New York, 2003.
3. H.S.Maiti, R.N.Basu, Mater. Res. Bull., 21 (1986) 1107.
4. D.Markovec, N.Ule, M.Drofenik, J. Am. Ceram. Soc., 84 (2001) 1273.
5. D.C.Sinclair, A.R.West, J. Appl. Phys., 66 (1989) 3850.
6. E.Barsoukov, J.R.Macdonald, Impedance Spectroscopy: Theory, Experiment, and Applications, John Wiley & Sons, 2005.
7. E.J.Abram, D.C.Sinclair, Journal of Electroceramics, 10 (2003) 165.
8. F.D.Morrison, D.C.Sinclair, A.R.West, J. Am. Ceram. Soc., 84 (2001) 531.
9. N.Hirose, A.R.West, J. Am. Ceram. Soc., 79 (1996) 1633.
10. F.D.Morrison, D.C.Sinclair, A.R.West, J.Am.Ceram.Soc. 84 (2001) 474.
11. A.R.West, D.C.Sinclair, N.Hirose, J. Electroceram., 1:1 (1997) 65.
12. J.R.Macdonald, Solid State Ionics, 176 (2005) 1961.
13. S.Komornicki, M.Radecka, M.Rekas, J. Mater. Sci., 12 (2001) 11.
14. W.H.Press, B.P.Flannery, S.A.Teukolsky, W.T. Vetterling, Numerical Recipes in C, Cambridge: Cambridge University Press, 1988.
15. M.P.Pechini, Method of preparing lead and alkaline earth titanates and coating method using the same to form a capacitor, US Patent No. 3.330.697, 1967.
16. B.Stojanović, C.R.Foschini, M.A.Zaghete, F.S.O.Vieira, M.Cilense, M.S.Castro, J.A.Varela, Mater. Eng., 12 (2001) 95.
17. D.Mančić, M.Radmanović, V.Paunović, V.Dimić, D.Stefanović, Sci. Sintering, 30 (1998) 53.
18. Lj.M.Živković, V.V.Paunović, N.Lj.Stamenkov, M.M.Miljković, Sci. Sintering, 38 (2006) 273.

Садржај: Диелектрична константа и диелектрични губици *La* допираног и недопираног BaTiO_3 испитивани су у функцији фреквенције и температуре. За проучавање електричних својстава BaTiO_3 коришћена је спектрална анализа импедансе у температурном опсегу од собне температуре до 350°C . *La* допирани и недопирани BaTiO_3 добијени модификованом Pechini методом синтеровани су 2 и 16 сати на 1300°C у атмосфери ваздуха. Спектри импедансе су анализирани на основу еквивалентних електричних кола која укључују отпорник, кондензатор и елементе са константном фазом (CPE). Најпогоднији модел за интерпретацију експерименталних резултата је еквивалентно коло које се састоји од два паралелна пара, отпорник-CPE елемент, везана редно. Допринос отпорности границе зрна укупној отпорности система је доминантан на нижој температури. Диелектрична константа допираног BaTiO_3 се креће у опсегу од 8000 до 12000 на 1 kHz, а диелектрични губици су мањи од 1%.

Кључне речи: *La-допиран BaTiO₃, спектрална анализа импедансе, еквивалентно коло, диелектрична константа.*
